Development of an Experimental Instrumentation Dedicated to ESD Testing and Measurement on Nanosatellites

Jean-Charles Matéo-Vélez, François Issac, Julien Jarrige, Yoann Bernard-Gardy, Gaël Murat, Jean Guérard, Denis Payan

Development of an Experimental Instrumentation Dedicated to ESD Testing and Measurement on Nanosatellites

Jean-Charles Mateo-Velez[1], François Issac[1], Julien Jarrige[1], Yoann Bernard-Gardy[1], Gaël Murat[1], Jean Guérard[1], and Denis Payan[2]

[1]ONERA-The French Aerospace Lab, 2 av Edouard Belin, 31055, Toulouse, France
[2]CNES, Toulouse, France

***Abstract*— Electrostatic discharges are known to be responsible for satellites anomalies during radiation belts disturbances. Few analyses have been performed so far on nanosatellites however. Ground testing is the most convenient method to evaluate spacecraft charging and its related effects in terms of electrostatic discharges and electromagnetic coupling. This paper presents an experimental instrumentation that is fully possible to adapt and embed on nanosatellite mockups.**

I. INTRODUCTION

Nanosatellites have become very common for the last decade to achieve a large variety of missions (in-orbit demonstration, science, commercial services). Since they have been developed mainly for large platforms, the design guidelines for assessing and preventing electrostatic discharges (ESD) and electromagnetic coupling (EMC) risks ([1]-[5]) must probably be adapted to the specificities of smaller platforms, including CubeSats. Low Earth orbit (LEO) charging issues occur in the auroral ovals during auroral electron injections ([6]-[7]). Geomagnetic substorms are known to increase the ESD risk at Geosynchronous (GEO) and middle Earth orbit (MEO) ([8]-[11]). On one hand, several factors decrease the surface ESD risks on nanosats. First, their orbits - mostly LEO - are less constraining than GEO and MEO in terms of electron fluxes about a few kilo-electronvolts of energy that are responsible for spacecraft charging. Second, the amplitude and duration of the blow-off and flash-over currents are reduced due to a smaller structure and to smaller solar panels. On the other hand, several factors increase the surface ESD risks on nanosats. First, the electronics sensitive to ESD transients and to EMC coupling through the harnesses are closer to the ESD location. Second, there is a relative lack of awareness of nanosatellites and CubeSat designers with respect to more conventional spacecraft.

To better assess ESD and related EMC risks, the blow-off and flash-over currents need to be measured with high precision and frequency bandwidth. ONERA and CNES have conducted research and development activities on nanosats charging for a few years. ONERA is currently preparing the CubeSIM payload (Sensing Impulses and Mitigation on CubeSat) for a flight on the ChaRging On CUbeSat satellite (CROCUS) in partnership with Centre Spatial de l'Ecole Polytechnique (CSEP).

Some important issues need to be solved to refine ESD characterization on nanosatellites during ground testing. First, avoid or at least limit any undesired side effects of the test setup on the ESD itself (triggering threshold, current propagation, absolute potential drop variations). Second, reduce the presence of nearby tank walls and other surfaces to limit their effects on the pre-discharge electric field, on blow-off electron trajectories and on the flash-over plasma expansion. Third, during the discharge, especially during the blow-off, limit the electrical ringing between the pre-charged equipement under test and the grounded support equipment (power supplies, capacitor representing the spacecraft capacitance with respect to the space plasma).

The solution adopted in this work is to « test as you fly », that is, with an electrically floating mockup. The test setup used in the present paper is described in a previous paper [12]. It consists in a series of instruments embedded in a nanosatellite mockup immersed in a vacuum chamber. The objective of this paper is to cross-compare and analyse the results of two instruments.

Section II of this paper describes the test setup. Section III presents a model of the measurement chain. Section IV presents the test and model results. Section V gives the conclusion and some perspectives of this work.

II. TEST SETUP

A. Nanosatellite structural models

Two nanosatellites mockups have been used. A 2.5U-like structural model (STM) and a 8U-like STM have been manufactured. They are composed of a conductive frame and of metallic plates. Two external panels are mounted on each STM to represent deployed solar panels. One side of those deployed panels is conductive. The other side is covered with insulators to mimick solar cell assemblies triple points.

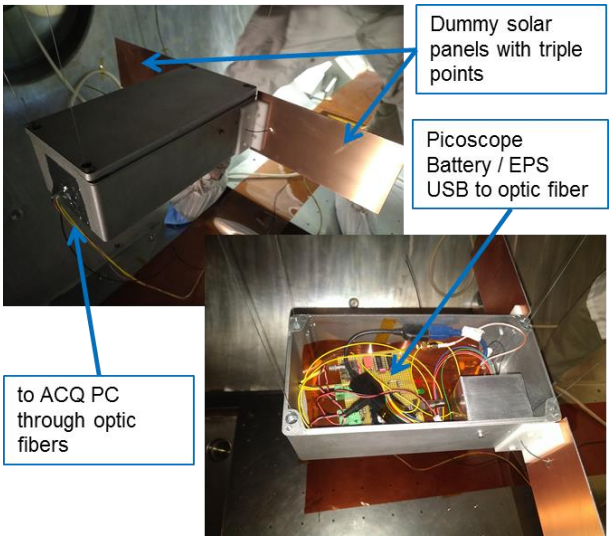

Fig. 1 - Pictures of the 2.5 U-like nanosatellite STM installed in the JONAS chamber

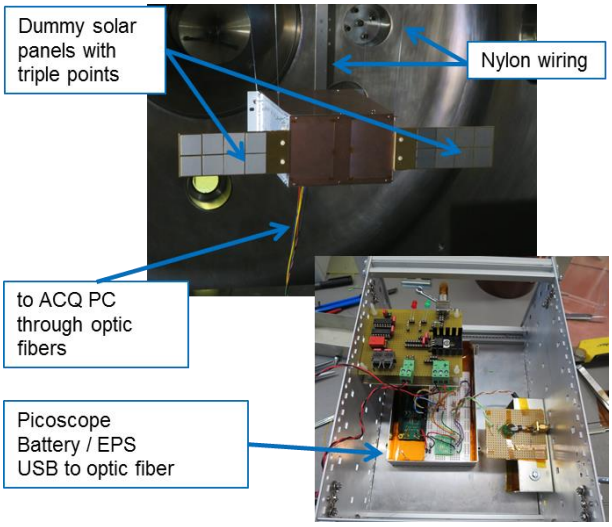

Fig. 2 - Pictures of the 8 U-like nanosatellite STM installed in the JONAS chamber

The nanosatellites STM are mounted one at a time at the center of the JONAS vacuum chamber located at ONERA [13]. They are fixed with nylon wires to maintain the electrical insulation with the tank ground. Fig. 1 and Fig. 2 show the mockups installed in the vacuum chamber.

B. *Instrumentation*

Fig. 3 presents the electrical setup installed in each STM. The electronics is powered by an electrical power board and a battery. A picoscope® PS4227 is connected to the laboratory acquisition system through an optical fiber. This scope maintains the electrical insulation of the mockup with respect to the tank ground. Channel 1 of the scope is connected to a 4.7 ohm resistor load connecting one external panel to the STM frame. That external panel is referred as the instrumented panel, in this paper. The other one is referred as the non-instrumented panel. A Pearson probe has also been used instead of the resistor to measure the current flowing between the panel and the frame. Channel 2 detects the electrical potential variations associated to ESDs. It is connected to the terminals of a 100 kohms resistor placed between the frame and a 10 cm-long conducting wire. This wire antenna is located outside and perpendicularly to the STM.

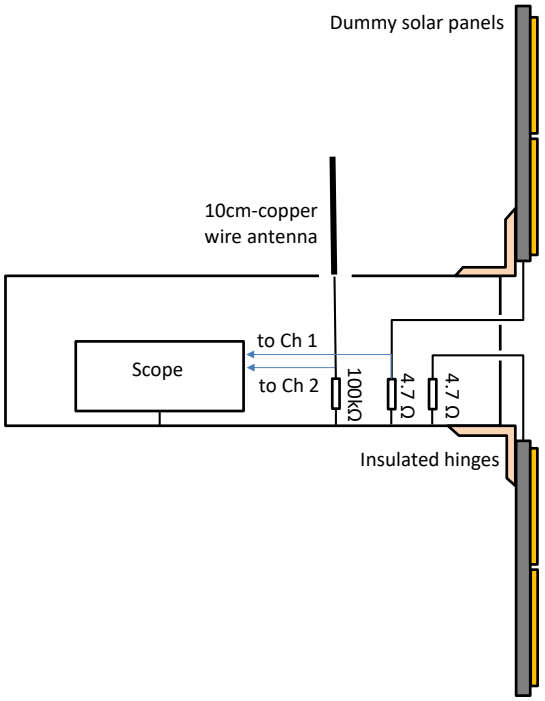

Fig. 3 – Electrical setup installed in the nanosatellite STM

C. *Charging Conditions*

Fig. 4 presents the conditions used to charge the nanosatellites STM. An electron gun produces an electron beam with energy from 5 to 15 keV and a current density from 0.1 up to 10 nA/cm^2. The electron beam makes the STM frame charge negative with respect to the ground.

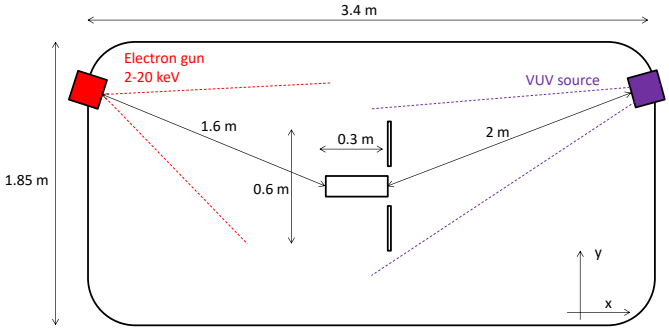

Fig. 4 – Charging conditions inside the JONAS chamber

A VUV source illuminates the opposite side mostly covered with insulators. The photons skip out electrons through photoemission. This produces the so-called inverted potential gradient (IPG) situation with negatively charged conductors and less negatively charged insulators at the triple points located on the external panels. This is known to facilitate surface ESDs.

III. MEASUREMENT MODELLING

The antenna measurement physical principle in the next figure, where Z_c is the load 100 kΩ resistor. The antenna voltage V_0 is proportional to the local electric field E.

$V_0 = -l_{eq} \times E$,

where l_{eq} is the antenna equivalent length.

E is assumed to be proportional to the nanosatellite mockup frame potential V_{sat}.

$E = k \times V_{sat}$,

where k is a constant that depends on nanosatellite geometry.

During an ESD, the satellite voltage evolves with the blow-off current I_{BO} according to the following equation

$C_{sat} \times dV_{sat}/dt = I_{BO}$

where C_{sat} is the nanosatellite capacitance with respect to the ground.

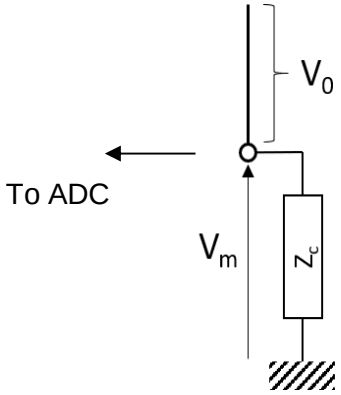

Fig. 5 – Antenna measurement schematical representation

The equivalent circuit of the antenna measurement is a high pass, see the next figure, where C is the antenna capacitance with respect to the nanosatellite frame.

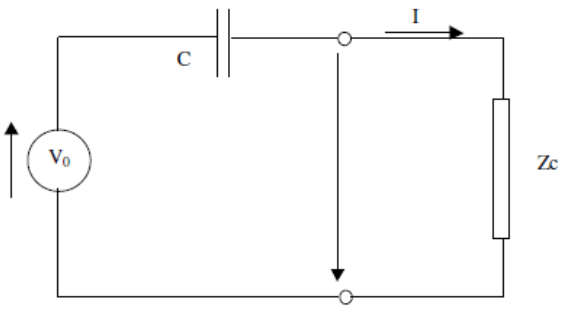

Fig. 6 – Antenna measurement equivalent electrical circuit

The relation between the antenna voltage and the measurement output V_m is :

$$V_m = \frac{1}{1 + \frac{1}{jZ_c C\omega}} V_0$$

For a signal with a characteristic frequency higher that the high pass cutoff frequency, the output voltage V_m tends to V_0. In this limit, the antenna signal simply writes:

$$\frac{dV_m}{dt} \approx k l_{eq} \frac{I_{BO}}{C_{sat}}$$

According to the Gauss theorem, we concluded that the blow-off current can be computed from the shunt resitor current, from the size of the different surfaces (platform, panels) and from the ESD location [12].

$I_{BO} = \alpha_1 \times I_{shunt}$,

when the ESD occurs on the instrumented panel, with I_{shunt} the current measured on the shunt resistor of the instrumented panel and α_1 a constant, and

$I_{BO} = -\alpha_2 \times I_{shunt}$,

when the ESD occurs anywhere else. The parameters l_{eq}, k, C_{sat}, α_1 and α_2 are constants that depends on the spacecraft dimensions and of materials arrangements.

IV. RESULTS

A total number of more than 50 ESDs have been analyzed. They were triggered at the triple points located on the external panels. We checked this with a video camera. The electrical signal quality is very good, with high precision and very limited current ringing. The current is clearly split into two phases. The first phase lasts from 0.5 to 1.5 µs with current amplitudes of about 20 to 400 mA. This is the blow-off current that discharges the STM negative potential with respect to the tank ground. The second phase concerns the development of a flash-over current that reduces the relatively positive voltage of surface insulators impacted by VUV. We checked this by measuring the surface potential on external panels before and after the ESDs with a contactless voltage probe. The flash-over current lasts often longer than 10 µs.

Fig. 7 shows an example of the transient signals measured during a blow-off discharge with a flash-over lasting more than the acquisition time period of 4 µs. The blow-off amplitude reaches 200 mA. The antenna voltage rises up to 15 V in absolute value. Both signals are well correlated.

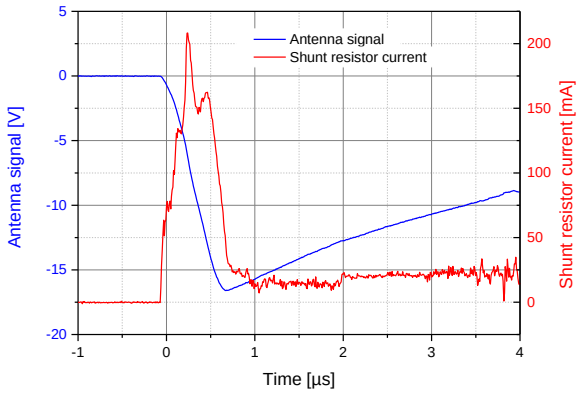

Fig. 7 – Example of transient signals measured during an ESD

The next figure (Fig. 8) presents the duration of the blow-off current as derived from the antenna signal and from the shunt current. The blow-off phase, which corresponds to the discharge of the satellite with respect to the environment, is characterized by a peak-shaped ESD current with a fast transient. The FO phase, which corresponds to neutralization of charges between the different parts of the satellite (dielectric surfaces and conductive structure), is characterized by a steady ESD current. Hence, the BO duration can be inferred from shunt resistor current, at the transition between the two phases. Concerning the antenna, the BO duration is estimated from the derivative of the signal ($dV_m/dt = 0$ at the end of the BO).

In the example of Fig. 7, the estimated BO duration is about 0.67 µs and 0.68 µs using the antenna and the shunt resistor, respectively. Overall, the blow-off duration measured in this test campaign ranges from 0.5 up to 1.5 µs.

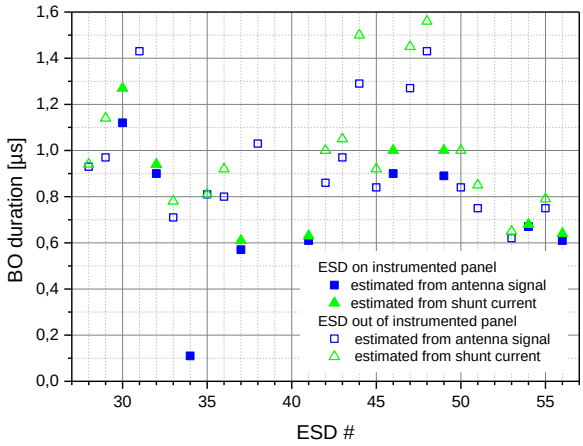

Fig. 8 – Blow off duration derived from the antenna signal and from the shunt current.

The next figures present the signals measured on the antenna during two ESDs that occurred on different places, i.e. one on the instrumented panel and the other one on the non-instrumented panel. As expected, the shunt current has opposite signature in terms of amplitude sign. The measured current amplitude is larger on ESDs occurring on the instrumented panel. The analysis of more than 50 ESDs showed that the above model is well satisfied with the following parameterizations:

$k \times l_{eq} \times \alpha_1 / C_{sat} = 2.33 \times 10^8$ F^{-1} and,

$k \times l_{eq} \times \alpha_2 / C_{sat} = 1.3 \times 10^9$ F^{-1}.

The model is illustrated in the next figures that represent the time evolution of the measured signals compared with the signals computed from the model, i.e. the antenna signal reconstructed from the measured shunt current and the shunt current reconstructed from the measured antenna signal.

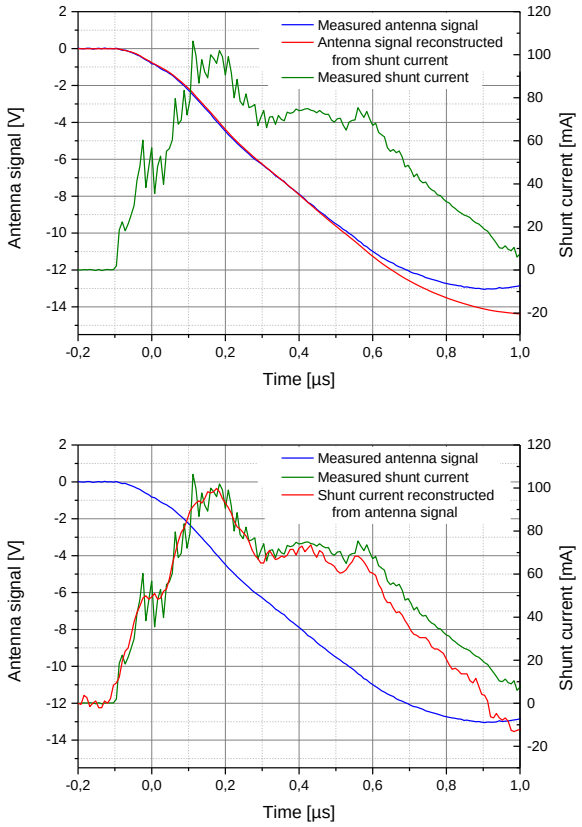

Fig. 9 – Antenna and shunt signals measured during an ESD that occurred on the instrumented panel, compared with (top) the antenna signal reconstructed from the measured shunt current and (bottom) the shunt current reconstructed from the antenna signal.

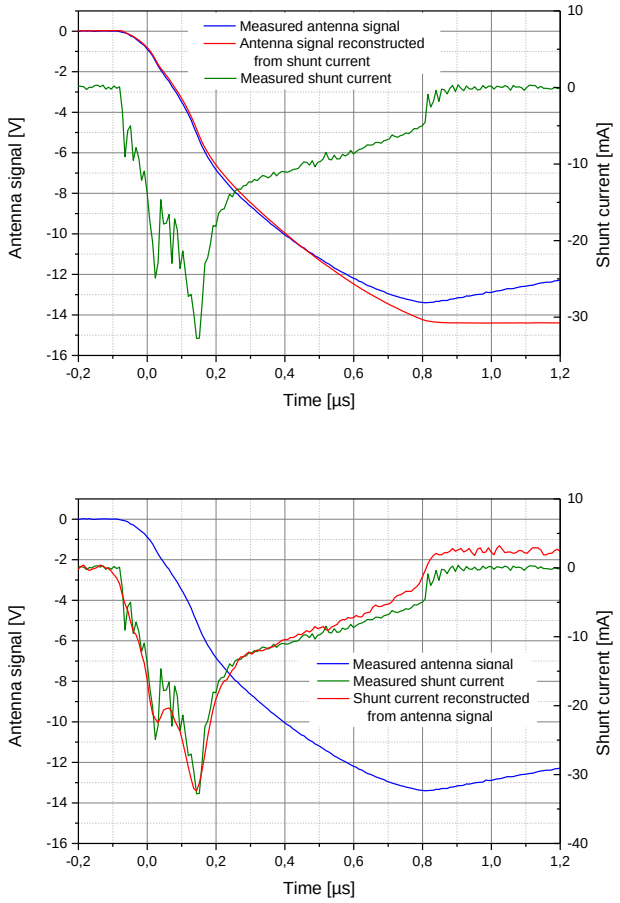

Fig. 10 – Antenna and shunt signals measured during an ESD that occurred on the non-instrumented panel, compared with (top) the antenna signal reconstructed from the measured shunt current and (bottom) the shunt current reconstructed from the antenna signal.

V. Conclusion

The test setup developed in this work is well suited to characterize ESD on nanosatellites because the electrical noise and disturbance are very limited by the disconnection between the tank ground and the mockups. No signal filtering is required. The blow-off peak current ranges from 10 to 400 mA and its duration from 0.5 to 1.5 µs under the test conditions.

The energy released is in the order of a few tens of micro-Joule which is enough to trigger bitflips in electronics. In addition, cable lengths on nanosatellites are significantly smaller than on more conventional spacecraft. That results on much less resistive and inductive losses on the path from the ESD site to the sensitive electronics. In many cases, cables on nanosats are less shielded. All this would suggest re-evaluating the risks with regards ESD/EMC.

The sensors used in this study are good candidates for in-flight ESD detection and waveforms meaurements with reasonable bandwidth (10-100 MHz) pending on nanosatellite specifications in terms of allocated power and data budget. It is quite easy to adapt these techniques to any nanosatelites mockups with their specificities (size, materials, electrical circuit, environmental conditions). The cross-calibration of the antenna and current measurements must be done with nanosatellites mockup representative of the flight models because their parameters are geometry dependent. It has been shown that the blow-off current could be reconstructed from the only antenna signal.

Additional sensors are under investigation to evaluate the pre-discharge nanosat potential and flash-over propagation. We plan to test miniaturized sensors embedded in the CubeSIM payload, currently in phase C, and to fly them on the CROCUS mission, currently in phase B.

Acknowledgment

The CubeSIM/CROCUS project is supported by ONERA ONSAT-1 research program. The authors thank the CROCUS team members at ONERA and at CSEP. The authors are grateful to helpful discussions with Laurent Garrigues from LAPLACE laboratory in Toulouse.

References

[1] C. K. Purvis, H. B. Garrett, A. C. Whittlesey, and N. J. Stevens, "Design Guidelines for Assessing and Controlling Spacecraft Charging Effects", NASA Technical paper, 1984, (No. NAS 1.60: 2361). Retrieved from https://ntrs.nasa.gov/citations/19840025381

[2] National Aeronautics and Space Administration (2022), Mitigating in space charging effects – a guideline (NASA standards NASA-HDBK-4002B). Retrieved from https://standards.nasa.gov/standard/nasa/nasa-hdbk-4002

[3] European Cooperation for Space Standardization (2019), Spacecraft charging (ECSS standard ECSS-E-ST-20-06C). Retrieved from https://ecss.nl/standard/ecss-e-st-20-06c-rev-1-spacecraft-charging-15-may-2019

[4] International Organization for Standardization (2011), Space systems — Space solar panels — Spacecraft charging induced electrostatic discharge test methods (ISO 11221:2011). Retrieved from https://www.iso.org/standard/50296.html

[5] European Cooperation for Space Standardization (2019), Assessment of space worst case charging handbook (ECSS standard ECSS-E-HB-20-06A). Retrieved from https://ecss.nl/home/ecss-e-hb-20-06a-assessment-of-space-worst-case-charging-handbook-15-may-2019.

[6] P. C. Anderson "Characteristics of Spacecraft Charging in Low Earth Orbit", J. Geophys. Res. **117** A07308 (2012), 10.1029/2011JA016875.

[7] A. I. Eriksson and J. E. Wahlund, "Charging of the Freja Satellite in the Auroral Zone", IEEE Trans. Plasma Sci. **34**, 2038 (2006), 10.1109/TPS.2006.883373.

[8] J. F Fennell, H. C. Koons, J. L. Roeder, and J. B. Blake, "Spacecraft Charging: Observations and Relationship to Satellite Anomalies", Defense Technical Information Center Report, 2001, ISBN: 1609-042X. Retrieved from https://apps.dtic.mil/sti/citations/ADA394826

[9] P. C. Anderson and H. C. Koons, "Spacecraft Charging Anomaly on a Low-Altitude Satellite in an Aurora", J. Spacecr. Rockets **33**, 734 (1996), 10.2514/3.26828.

[10] D. C. Ferguson, W. F. Denig, and J. V. Rodriguez, "Plasma Conditions During the Galaxy 15 Anomaly and the Possibility of ESD from Subsurface Charging", proceedings of the 49th

AIAA Aerospace Sciences Meeting, Orlando, FL, Januray 2011, paper AIAA-2011-1061, 10.2514/6.2011-1061.

[11] N. Ahmad, D. Herdiwijaya, T. Djamaluddin, H. Usui, and Y. Miyake,"Diagnosing Low Earth Orbit Satellite Anomalies Using NOAA-15 Electron Data Associated with Geomagnetic Perturbations", Earth Planet Space **70**, 91 (2018), ISBN: 1343-8832, 10.1186/s40623-018-0852-2.

[12] Bernard-Gardy, Y., et al., "Innovative technique for electrostatic discharges characterization on a floating nanosat mockup " to be published in Jour. Spacecraft and Rockets

[13] Mateo-Velez, J. C., et al. "Ground Plasma Tank Modeling and Comparison to Measurements", IEEE Trans. Plasma Sci. 36, 2369 (2008).